Published in final edited form as:
*J Immunol*. 2009 November 15; 183(10): 6478–6488. doi:10.4049/jimmunol.0901615.

# $Ca^{2+}$ Waves Initiate Antigen-Stimulated $Ca^{2+}$ Responses in Mast Cells

**Roy Cohen**[*], **Alexis Torres**[*], **Hong-Tao Ma**[†], **David Holowka**[*,1], and **Barbara Baird**[*]

[*]Department of Chemistry and Chemical Biology, Cornell University, Ithaca, NY, 14850 USA

[†]Laboratory of Molecular Immunology, National Heart, Lungs and Blood Institute, National Institute of Health, Bethesda, MD, 20892 USA

## Abstract

$Ca^{2+}$ mobilization is central to many cellular processes, including stimulated exocytosis and cytokine production in mast cells. Using single cell stimulation by IgE-specific antigen and high speed imaging of conventional or genetically-encoded $Ca^{2+}$ sensors in RBL and bone marrow-derived rat mast cells, we observe $Ca^{2+}$ waves that originate most frequently from the tips of extended cell protrusions, as well as $Ca^{2+}$ oscillations throughout the cell that usually follow the initiating $Ca^{2+}$ wave. In contrast, antigen conjugated to the tip of a micropipette stimulates local, repetitive $Ca^{2+}$ puffs at the region of cell contact. Initiating $Ca^{2+}$ waves are observed in most RBL cells stimulated with soluble antigen, are sensitive to inhibitors of $Ca^{2+}$ release from ER stores and to extracellular $Ca^{2+}$, but they do not depend on store-operated $Ca^{2+}$ entry. Knockdown of TRPC1 and TRPC3 channel proteins by shRNA reduces the sensitivity of these cells to antigen and shifts the wave initiation site from protrusions to the cell body. Our results reveal spatially encoded $Ca^{2+}$ signaling in response to immunoreceptor activation that utilizes TRPC channels to specify the initiation site of the $Ca^{2+}$ response.

### Keywords

IgE receptors; $Ca^{2+}$ puffs; $Ca^{2+}$ oscillations; GCaMP2; TRPC channels

## INTRODUCTION

Changes in intracellular $Ca^{2+}$ play significant roles in numerous cellular responses such as secretion, gene expression, and cell migration. These cellular functions require spatial and temporal regulation of cytosolic $Ca^{2+}$ (1,2). Among these regulated events are $Ca^{2+}$ puffs, waves, and regenerative oscillations that mediate localized cellular responses and support transfer of information across the cell and organelles (3).

$Ca^{2+}$ waves were first characterized in Xenopus oocyte fertilization (4), and they have since been identified in excitable (5) and nonexcitable cell types, including hepatocytes (6), HeLa cells (7), and neutrophils (8). In myocytes, $Ca^{2+}$ waves were shown to initiate from elementary $Ca^{2+}$ events called "$Ca^{2+}$ sparks" (9), and are thought to propagate through the cytosol by calcium-induced calcium release from ER stores (10). $Ca^{2+}$ waves are frequently initiated by activation of plasma membrane receptors that stimulate $Ca^{2+}$-dependent signaling within the cell (11). Similar mechanisms may be involved in stimulating $Ca^{2+}$ puffs and maintaining the propagation of $Ca^{2+}$ waves in non-excitable cells (3,12).

[1]To whom correspondence should be addressed: dah24@cornell.edu, 607-255-4848 .

However, $Ca^{2+}$ waves in response to immunoreceptor signaling have not been previously reported.

$Ca^{2+}$ oscillations have been characterized in many cell types, including RBL-2H3 mast cells (13,14) where they have been temporally correlated with degranulation events (15,16). $Ca^{2+}$ oscillations are sustained by store-operated $Ca^{2+}$ entry (SOCE), other ion channels, as well as membrane potential (17).

Mast cells play key roles in the inflammatory process in both innate and adaptive immune responses (18). In the latter, binding of multivalent antigen to receptor-associated IgE aggregates this receptor, FcεRI, which causes mast cell activation, resulting in $Ca^{2+}$ mobilization and consequent exocytotic release of mediators of allergy and inflammation (19). RBL-2H3 cells are immortalized mucosal mast cells that have been utilized for extensive biochemical and cell biological investigations of mast cell function (20-22).

In the present study, we used high-speed confocal imaging to investigate cytoplasmic $Ca^{2+}$ dynamics activated via FcεRI in RBL cells and in rat bone marrow-derived mast cells (BMMCs), which are also mucosal in character (23). We find that $Ca^{2+}$ responses to soluble antigen initiate in the form of a wave that begins most frequently at the tip of an extended cell protrusion and propagates throughout the entire cell in several seconds. In contrast, localized delivery of antigen attached to the tip of a micropipette results in repetitive, localized $Ca^{2+}$ puffs that infrequently develop into propagated waves. Our results provide evidence that $Ca^{2+}$ wave initiation from extended protrusions depends on $Ca^{2+}$ influx via TRPC channels leading to the onset of SOCE-dependent $Ca^{2+}$ oscillations and mast cell activation.

## MATERIALS AND METHODS

### cDNA plasmids

The GCaMP2 construct (24) was provided by Dr. M. Kotlikoff, Cornell University College of Veterinary Medicine. shRNA plasmids targeting TRPC channels (TRPC1, TRPC3, TRPC5, TRPC7 and GFP control) were characterized in RBL cells as previously described (25).

### Chemicals and reagents

Fluo4AM and Fluo5FAM were purchased from Invitrogen/Molecular Probes (Eugene, OR). U73122, D-sphingosine, thapsigargin, A23187, 2-aminoethyldiphenyl borate (2-APB), and $GdCl_3$ were from Sigma-Aldrich (St. Louis, MO). N,N'-dimethylsphingosine (DM-sphingosine) was from Avanti Polar Lipids (Alabaster, AL).

### Cells

RBL-2H3 cells (26) were maintained in monolayer culture in Minimum Essential Medium supplemented with 20% fetal bovine serum (Atlanta Biologicals, Norcross, GA, USA) and 10 μg/ml gentamicin sulfate. All tissue culture reagents were obtained from Gibco (Grand Island, NY, USA) unless otherwise noted. Rat BMMCs were differentiated from femur-derived stem cells of Lewis strain rats by culturing for 14-28 days in the presence of rat stem cell factor (50 ng/ml) and rat IL-3 (100ng/ml) as previously described (27). Cells were harvested 3–5 days after passage and plated overnight in MatTek coverslip dishes in complete medium for experiments with Fluo-5F AM loading. For experiments with GCaMP2 as the $Ca^{2+}$ indicator, $5 \times 10^6$ RBL-2H3 cells were electroporated in 0.5 ml of cold electroporation buffer (137mM NaCl, 2.7mM KCl, 1mM $MgCl_2$, 1mg/ml glucose, 20mM Hepes, pH=7.4) with 5-8 μg of plasmid DNA at 280V and 950μF using Gene Pulser X (Bio-

Rad), then plated onto MatTek dishes (~500,000 cells/plate). Cells were sensitized with 0.5 μg/ml anti-2,4-dinitrophenyl (DNP) IgE (28) during overnight cell culture incubation. Under these conditions, the cell transfection efficiency with GCaMP2 is typically 20-30%.

For experiments with TRPC shRNA constructs, plasmids containing these sequences (Origene Technologies) were co-electroporated with that for GCaMP2 using 20 μg of TRPC shRNA plasmid and 8 μg of GCaMP2 plasmid for $5 \times 10^6$ cells. No effect of these plasmids on cell viability was detected.

For characterization of rat BMMCs, differentiated cells were labeled with 2 μg/ml Alexa488-IgE (29) for 2 hr at 37°C, then washed and fixed in 4% (w/v) p-formaldehyde and 0.1% (w/v) glutaraldehye for 20 min at room temperature. Fixed cells were further labeled in 10 mg/ml BSA/PBS/0.01% $NaN_3$ with 3 μg/ml monoclonal anti-α-galactosyl $GD_{1b}$ ganglioside AA4 (30), followed by 10 μg/ml Alexa555-goat anti-muIg$G_1$ (Invitrogen Corp.). Washed, labeled cells were imaged as previously described (31).

## Live cell calcium imaging

24 hours after transfection, cells were washed with buffered salt solution (BSS: 135mM NaCl, 5mM KCl, 1.8mM $CaCl_2$, 1mM $MgCl_2$, 1 mg/ml glucose, 20mM Hepes, pH=7.2-7.4, 1mg/ml BSA) and imaged using a heated (37°C) 63X (NA=1.4) oil immersion objective on a Zeiss Meta 510 confocal microscope. GCaMP2, Fluo-4 or Fluo-5F were excited using the 488 nm line of a krypton/argon laser and viewed with a 505–530 band-pass filter. In experiments using Fluo-4 AM or Fluo-5F AM, cells were labeled by incubating with 0.5 μM (RBL cells) or 2.5 μM (rat BMMCs) of the indicator in BSS in the presence of 2.5 mM sulfinpyrazone for 30 min in 37°C (5 min for rat BMMCs), then washed and imaged in BSS.

Cells expressing GCaMP2 or loaded with Fluo dyes were approached with a ~5 μm diameter pulled glass capillary, typically positioned within 100 microns from the cell and pre-filled with stimulating solution. Cells were imaged at 10-30 Hz while applying a puff of 10 seconds/5psi from the pipette. Pressure and duration of stimulation was controlled by a Picospritzer III (FMI Medical Instruments, GmbH). Pharmacological reagents were added to the dishes just prior to initiating data collection (see Results). For some experiments, DNP-BSA (Ag) or unmodified BSA was covalently coupled to the micropipette surface using chemical treatments and procedure previously described for covalent attachment of proteins to patterned surfaces (32).

## Data analysis

Images of individual cells are representative from multiple experiments. Off line image analysis was carried out using Zeiss LSM image analysis software (Carl Zeiss, Inc) and ImageJ (NIH). Changes in fluorescence (F) were normalized by the initial fluorescence ($F_0$) and are expressed as ΔF.

Unless stated otherwise, cells that displayed any type of $Ca^{2+}$ elevation including $Ca^{2+}$ puffs upon stimulation were counted as responding cells. Wave occurrence was calculated as the percentage of cells with a detectable $Ca^{2+}$ wave, compared to the total number of responding cells in a given experimental condition. The lag time before $Ca^{2+}$ wave initiation was measured from the initiation of the pulse of Ag or other stimulus. Statistical analysis of $Ca^{2+}$ oscillations was carried out by counting and averaging the oscillatory peaks during the first 2 minutes of stimulation, including the initiating wave. Wave propagation velocity was measured as the time (number of frames x time per frame) for spreading of the wave-front across a cell of measured dimension. Unless otherwise stated, all data are presented as mean ± SEM. For each of the experiments, the number of cells analyzed (n) is presented in the

text. Data were processed and plotted using Origin 8 (OriginLab) and Excel (Microsoft Corp.). Statistical comparisons between experiments were preformed using Students t-test.

## RESULTS

### $Ca^{2+}$ mobilization events in individual RBL mast cells

To observe the earliest steps in the responses of RBL mast cells to stimulation of IgE receptors by multivalent antigen, we delivered a short (10 sec) pulse of antigen (Ag) via a micropipette placed within 100 μm of the cell while imaging changes in cytosolic $Ca^{2+}$ (Figure 1A). For most experiments, we used the genetically encoded $Ca^{2+}$ indicator, GCaMP2, which has a moderate $K_d$ (~350 nM) with rapidly reversible kinetics (33). GCaMP2 is brighter than wild type GFP, maintains a 5-fold dynamic range, displays very low pH sensitivity and is fully functional at 37°C (24, 33).

Using high imaging rates of 10-30 frames per second, we observe two major types of spatially and temporally resolved $Ca^{2+}$ mobilization dynamics in individual cells as illustrated in Figure 1B and Supplemental Movie 1. Stimulation of cells with a saturating concentration of Ag (1.7 μg/ml in the pipette) resulted in more than 90% of the cells responding with a $Ca^{2+}$ wave that initiated a global $Ca^{2+}$ response. This initiating $Ca^{2+}$ wave followed a lag period of ~20 seconds, on average, after starting the Ag pulse (Table I). As illustrated in Figure 1B and will be discussed below, the $Ca^{2+}$ wave usually initiates from the tip of an extended cell protrusion and propagates down the length of the cell body. The site of wave initiation does not detectably correlate with the location of the micropipette relative to any particular part of the cell. $Ca^{2+}$ waves also initiated most frequently from the tips of extended protrusions in response to bath addition of antigen, but the lag time for wave initiation was more variable under these conditions (data not shown).

In most cells the $Ca^{2+}$ wave is followed by a second manifestation of calcium dynamics – regenerative $Ca^{2+}$ oscillations that occur throughout the cell body as previously described for these cells (13,14,16). Although not seen in the cell shown in Figure 1B, $Ca^{2+}$ oscillations often extend throughout the length of the cell, including protrusions. Spatial and temporal resolution of these two processes are shown in Figure 1C as time traces for the tip of the protrusion (red trace and red region of interest (ROI) in inset) and the cell body (black trace, yellow ROI in inset) for the cell in Figure 1B. In some cells, we observed localized $Ca^{2+}$ puffs prior to the initiation of waves; however, these were infrequent under conditions of optimal stimulation (see below).

We used Fluo4 and Fluo5F to confirm our main results for these $Ca^{2+}$ dynamics. Fluo4 and GCaMP2 have similar affinities for $Ca^{2+}$, but the fluorescence response kinetics are approximately an order of magnitude slower for the GFP-based sensor. As shown in Supplemental Figure S1, despite this slower response time for GCaMP2, $Ca^{2+}$ wave velocities measured using GCaMP2 were significantly higher than those measured with Fluo4, indicating that GCaMP2 kinetics are not a limiting factor in our measurements. The percentage of cells exhibiting $Ca^{2+}$ waves detected by Fluo4 is smaller, and the observed waves initiate after a longer lag time and exhibit slower propagation velocities. Interestingly, fewer $Ca^{2+}$ oscillations were detected with both Fluo4 and Fluo5F compared to GCaMP2, possibly due to $Ca^{2+}$ buffering effects of these organic dyes, which are difficult to load into cells at controlled concentrations. Overall, we found GCaMP2 to be most useful for our experiments.

Although there are cell-to-cell differences in appearance and characteristics of Ag-stimulated $Ca^{2+}$ waves and subsequent oscillations in the RBL cells, we found that several characteristics are highly consistent for a particular concentration of Ag. These include the

lag time to initiation of the first $Ca^{2+}$ peak, the wave velocity, and the frequency (number observed in 2 minutes) of the oscillations (Table I).

### Cellular protrusions are the primary initiation sites for $Ca^{2+}$ wave responses to Ag stimulation in RBL cells

As summarized in Figure 2B, ~90% of the cells responded to Ag (1.7 μg/ml) with a propagating $Ca^{2+}$ wave, whereas for the remaining ~5-10% of the responding cells we detected a non-directional, global elevation in cytoplasmic $Ca^{2+}$. Although stimulated influx of extracellular $Ca^{2+}$ is required for cellular degranulation, we observed wave initiation with similar frequency in the presence and absence of extracellular $Ca^{2+}$, suggesting that $Ca^{2+}$ influx is not necessary for $Ca^{2+}$ wave generation and propagation. However, a clear difference in the spatial localization of wave initiation is observed, depending on the presence or absence of extracellular $Ca^{2+}$. As illustrated in Figure 2A and Supplemental Movie 2, and summarized in Figure 2B, wave initiation in the absence of extracellular $Ca^{2+}$ occurs most frequently at a site in the cell body, with less frequent (<30%) initiation in elongated protrusions. This contrasts with extracellular $Ca^{2+}$ at 2-10mM when the majority of waves stimulated by Ag initiate near the tips of these protrusions (Fig. 1 and Fig. 2B). Similarly, reducing the driving force for $Ca^{2+}$ influx by depolarizing the cells with addition of 50 mM KCl prior to Ag stimulation also decreases the incidence of waves initiating from elongated protrusions to <30% (Table I). These results suggest that initiation of $Ca^{2+}$ waves from elongated protrusions depends on $Ca^{2+}$ influx.

Extended protrusions are common morphological features of RBL mast cells that are readily observed at low cell densities. They develop several hours after cell attachment and define an axis of cell migration (J. Lee and D. Holowka, unpublished results). Similar protrusions are frequently observed with mucosal mast cells imaged in vivo (for examples see: (34-37).

We found that substitution of extracellular $Ca^{2+}$ with equimolar concentrations of $Ba^{2+}$ or $Sr^{2+}$ prior to stimulation did not markedly alter either the percentage of cells with Ag-stimulated waves or initiation from elongated protrusions (Table I). The velocity of wave propagation was reduced by ~40% in the absence of extracellular $Ca^{2+}$, whereas substitution of $Ca^{2+}$ by $Ba^{2+}$, which is not taken up into stores by SERCA pumps (38), does not alter wave velocity (Table I). These results are consistent with wave initiation from protrusions by a $Ca^{2+}$ influx component and propagation by $Ca^{2+}$-dependent $Ca^{2+}$ release from intracellular stores (10,39). Interestingly, we find that the lag time for wave appearance following Ag stimulation was longer in the absence of extracellular $Ca^{2+}$ (Table I), but was not changed when $Ca^{2+}$ was substituted with $Ba^{2+}$ or $Sr^{2+}$. This delay could be attributed to a reduced “ignition” capacity of the calcium response in the absence of a $Ca^{2+}$ influx, and is further discussed below.

In addition to the observed effects on $Ca^{2+}$ waves, the absence of extracellular $Ca^{2+}$ substantially decreases the frequency of subsequent $Ca^{2+}$ oscillations (Figure 2C), as expected from the dependence of these oscillations on sustained, store-operated $Ca^{2+}$ influx (17). Substitution of $Ba^{2+}$ or $Sr^{2+}$ for extracellular $Ca^{2+}$ markedly reduces the frequency of oscillations (Table I), consistent with the high selectivity of CRAC channels to $Ca^{2+}$ over $Ba^{2+}$ or $Sr^{2+}$ (40, 41).

We compared the dynamic features of Ag-stimulated $Ca^{2+}$ responses in RBL cells to those observed upon stimulation with either the SERCA inhibitor thapsigargin (TG) or the $Ca^{2+}$ ionophore, A23187. As illustrated by individual time traces in Figure 2D and summarized in figure 2F, the oscillatory dynamics of Ag responses are largely absent from responses to TG and A23187. For TG at 1μM in the pipette, a transient increase in cytoplasmic $Ca^{2+}$ was typically observed, followed by a more sustained increase that depends on extracellular

$Ca^{2+}$. As summarized in Figures 2E, $Ca^{2+}$ waves are less frequently observed with TG stimulation, but, when observed, waves usually initiate from extended protrusions. For stimulation by A23187 at 20 μM in the pipette, $Ca^{2+}$ responses initiate as a wave in only about 40% of the cells, and this occurs very infrequently from extended protrusions (Figure 2E). Furthermore, when the response to A23187 does initiate as a $Ca^{2+}$ wave, the wave velocity is substantially slower than observed in cells stimulated by high concentration of Ag or TG (see Table I). Similar to TG, A23187-mediated elevation in cytoplasmic $Ca^{2+}$ does not cause oscillatory behavior in the majority of the stimulated cells (Figures 2D and F).

In summary, elevations in cytoplasmic $Ca^{2+}$ caused by either ionophore or TG-induced release from stores can also initiate $Ca^{2+}$ waves from discrete sites along the plasma membrane, but with lower probability. These results further indicate that cytoplasmic $Ca^{2+}$ oscillations such as those initiated by Ag can be uncoupled from $Ca^{2+}$ wave initiation caused by these non-receptor means of cell activation.

## Characterization of the $Ca^{2+}$ response in rat BMMCs

To evaluate whether the characteristics of $Ca^{2+}$ responses that we observe for RBL-2H3 cells are general for mast cells, BMMCs were differentiated from Lewis rats as previously described (27). When plated overnight on glass slides in MatTek dishes, these cells attach firmly and frequently exhibit extended protrusions, similar in morphology to RBL cells. We confirmed their identity by labeling with Alexa 488-IgE and AA4 mAb that labels a mast cell specific ganglioside (42,43;supplemental figure S4) as well as by staining granules with Alcian blue ((44); data not shown). BMMCs sensitized with IgE and labeled with Fluo-5F were stimulated as described above for RBL cells. As shown in Figure 3, we find that the majority of responding BMMCs exhibit initiating $Ca^{2+}$ waves that often begin in extended protrusions, similar to $Ca^{2+}$ waves observed in RBL cells. Also similar to $Ca^{2+}$ responses in RBL cells, oscillations throughout the cytoplasm often follow the initial, propagating $Ca^{2+}$ wave (Fig. 3b). These findings indicate that antigen-stimulated $Ca^{2+}$ responses in rat BMMCs, including $Ca^{2+}$ waves that initiate from specific morphological features, are similar to those characterized in cultured RBL mast cells.

## Antigen dose dependence and spatial localization

To assess further the nature and function of the $Ca^{2+}$ waves, we characterized the dose dependence of Ag-stimulated $Ca^{2+}$ responses in RBL cells detected with GCaMP2 (Supplemental Figure S2). More than 90% of the cells respond to antigen doses in the range of 17-1700 ng/ml in the pipette, and more than 50% of the cells respond at the lowest dose tested, 1.7 ng/ml (Figure S2A). $Ca^{2+}$ waves were observed in a similarly high percentage of the responding cells (≥80%) at all doses tested, but $Ca^{2+}$ waves initiate more frequently at extended protrusions at the lowest Ag dose (Figure S2C). Wave velocity was found to be dependent on the concentration of Ag (Figure S2B), and longer lag times between antigen addition and the first $Ca^{2+}$ response were observed at lower Ag doses (Figure S2D), but the frequency of $Ca^{2+}$ oscillations changes little over the four orders of magnitude of Ag concentration (Figure S2E).

$Ca^{2+}$ puffs are localized and transient elevations in cytoplasmic $Ca^{2+}$ that may serve as a priming mechanism for wave initiation and subsequent oscillations (39,45,46). Stimulated $Ca^{2+}$ puffs are observed less often than $Ca^{2+}$ waves at higher doses of antigen, but appear more often at the lowest concentration of Ag tested (Figure S2F). Consistent with these observations, $Ca^{2+}$ puffs may represent sub-threshold activation of the cells and production of insufficient amounts of $IP_3$ to generate a propagated $Ca^{2+}$ elevation and a global $Ca^{2+}$ response.

Interestingly, when antigen is covalently coupled to the tip of a micropipette and delivered locally by cell contact, we usually observe a series of stimulated $Ca^{2+}$ puffs that frequently occur near the point of contact. As illustrated in Figure 4, two different responses are typical: In one case, repetitive puffs are observed at relatively regular time intervals, often over several minutes of contact, but they fail to propagate as waves or global cellular $Ca^{2+}$ elevation for more than several microns (Fig. 4A). Alternatively, $Ca^{2+}$ puffs initiated by local contact of the antigen-coated pipette occasionally propagate as waves that traverse the length of the cell (Fig. 4B). Under these conditions of stimulation, contact at a cell protrusion did not significantly increase the probability of wave propagation. $Ca^{2+}$ puffs or waves were observed in more than 85% of cells contacted by DNP-BSA coated tips in both the presence and absence of extracellular $Ca^{2+}$ (Fig. 4C) and only rarely in cells contacted by unconjugated micropipettes or those conjugated with unmodified BSA (Fig. 4C). Moreover, $Ca^{2+}$ puffs were just as frequent when cells were locally stimulated with DNP-BSA conjugated micropipettes in the absence of extracellular $Ca^{2+}$ (Fig. 4C). These results suggest that the localized responses are mediated by release of $Ca^{2+}$ from internal stores, rather than by $Ca^{2+}$ influx. Moreover, localized activation of FcεRI can stimulate spatially restricted $Ca^{2+}$ responses, and, in this situation, the site of $Ca^{2+}$ response initiation is determined by the location of receptor stimulation.

These results show that the localized $Ca^{2+}$responses can be initiated by localized receptor stimulation, and these responses are apparently independent of $Ca^{2+}$ influx. Overall, these results show that $Ca^{2+}$ responses to soluble Ag begin most frequently as $Ca^{2+}$ waves that are propagated from initiation sites near the tips of extended protrusions, whereas those stimulated by locally applied micropipette-conjugated antigen are initiated at the site of stimulation, and are more commonly manifested as repetitive $Ca^{2+}$ puffs that less frequently evolve into $Ca^{2+}$ waves.

## Pharmacologic characterization of $Ca^{2+}$ dynamics

In initial efforts to identify molecular components of Ag-stimulated waves and oscillations, we investigated the effects of several different inhibitors of $IP_3$ production and modulators of $Ca^{2+}$ influx. As summarized in figure 5 and in Table I, the phospholipase C **(**PLC) inhibitor, U73122, reduces the percentage of cells showing $Ca^{2+}$ responses with a sharp dose dependence that is half maximal between 2 and 2.5 μM. U73122 also reduces the percentage of cells with an initiating $Ca^{2+}$ wave with a similar dose-dependence, suggesting that Ag-stimulated $Ca^{2+}$ waves depend on $IP_3$ and/or diacylglycerol production (Figure 5). In this dose range, U73122 is relatively selective for PLC isoforms in these cells, but at higher doses other proteins are also affected by this maleimide derivative (47). As summarized in Figure 5, Ag-stimulated $Ca^{2+}$ oscillations are inhibited with a similar dose-dependence, consistent with $IP_3$-dependent intracellular $Ca^{2+}$ increase as a necessary precursor to SOCE (48).

2-APB was initially described as a non-competitive antagonist of $IP_3$ receptor ($IP_3R$)-mediated $Ca^{2+}$ release by microsomal preparations (49), and it was subsequently shown to inhibit SOCE in T cells at concentrations in the range of 10-50μM (50). In RBL cells, 2-APB at concentrations up to 40μM has no effect on Ag-stimulated $Ca^{2+}$ release from stores in the absence of extracellular $Ca^{2+}$, indicating that it fails to inhibit $IP_3R$-mediated $Ca^{2+}$ release from stores in these cells (D. Holowka, unpublished results). As summarized in Figure 5, addition of 20μM 2-APB prior to Ag stimulation does not significantly reduce the percentage of responding cells (Figure 5A), or the percentage of cells that exhibit wave initiation (Figure 5B). In contrast, 20μM 2-APB strongly inhibits $Ca^{2+}$ oscillations subsequent to wave initiation (Figure 5C), consistent with its inhibitory effect on SOCE that contributes to $Ca^{2+}$ oscillations in these cells (51-53)

A previous study by Penner and colleagues (54) identified both D-sphingosine and N,N-dimethylsphingosine (DMS) as effective inhibitors of $IP_3$ and TG-elicited $Ca^{2+}$ release-activated $Ca^{2+}$ (CRAC) channel activation in RBL cells. As summarized in Figure 5B and Table I, we found that 8 μM D-sphingosine or 8 μM DMS strongly inhibits $Ca^{2+}$ wave initiation. Earlier studies suggested that DMS prevents $Ca^{2+}$ responses by inhibition of sphingosine kinase (55,56). However, this mechanism is unlikely for the inhibition we observe because D-sphingosine is a substrate of this enzyme family. In other studies, we have evidence that these basic amphiphiles inhibit $Ca^{2+}$ responses by electrostatically neutralizing negatively charged phospholipids at the inner leaflet of the plasma membrane ((57); N. Smith et al., manuscript in preparation). The small percentage of cells that do respond in the presence of D-sphingosine appear to have oscillation frequencies similar to untreated cells (Figure 5C), suggesting that this aspect of SOCE is less potently inhibited than wave initiation. These results identify these sphingosine derivatives as effective inhibitors of the earliest manifestations of $Ca^{2+}$ responses to Ag in these cells.

We further tested the effects of inhibitors of dihydropyridine-sensitive $Ca^{2+}$ channels on Ag-stimulated $Ca^{2+}$ wave initiation in RBL cells (58). As summarized in Figure 5, we observed a modest (~30%) reduction of wave initiation from extended protrusions by 10 μM nifedipine, but no effects of other L channel inhibitors such as Bay K (+) were detected (data not shown), suggesting that the effect of nifedipine observed may be due to non-specific inhibition of $K^+$ channels resulting in cell depolarization (59,60). To investigate further a possible contribution of CRAC conductance to wave generation, we examined the effects of $Gd^{3+}$ on $Ca^{2+}$ responses to Ag. Pre-addition of 10 μM $Gd^{3+}$ strongly inhibits $Ca^{2+}$ oscillations in response to Ag (Fig. 5C), consistent with inhibition of SOCE (61), but it causes only a small reduction in the percentage of waves initiating from extended protrusions (Figure 5B). These results are consistent with those obtained with 2-APB that indicate little or no contribution of CRAC channels to Ag-stimulated wave initiation. Because $Ca^{2+}$ influx contributes to the spatial localization of $Ca^{2+}$ wave initiation from protrusions (Fig. 2), these results suggest that $Ca^{2+}$ channels other than CRAC or voltage gated channels contribute to this process.

## Involvement of TRPC channels in the initiation of $Ca^{2+}$ waves from protrusions

Expression of TRPC channels in RBL cells was demonstrated by Pizzo et al. (62) and more recently by Ma et al (25). TRPC channels have been identified as receptor activated $Ca^{2+}$ channels, and we investigated the contribution of TRPC channels to wave initiation by IgE-FcεRI in RBL mast cells using shRNA sequences targeting TRPC1, TRPC3, TRPC5 and TRPC7 to knock down expression of these proteins (25). For these experiments, RBL cells were co-transfected with the $Ca^{2+}$ indicator GCaMP2 and one of the TRPC targeting shRNA plasmids as described in Materials and Methods. We found that transfection with TRPC1 shRNA and, to a lesser extent, with TRPC3 shRNA reduces the responsiveness of the cells to a low concentration of Ag compared to cells expressing a mock shRNA sequence, and these effects are particularly notable if cells responding with $Ca^{2+}$ puffs are not included in the count (Figure 6A). As shown in Supplemental Figure S3, we observe ~50% reduction in TRPC1 expression due to shRNA transfection in these cells, similar to previous results (25). This value represents a lower limit to the knockdown of TRPC1 cell expressing GCaMP2, which is co-transfected with the shRNA constructs. Under these knock down conditions, we did not observe a significant reduction in the percentage of cells responding to Ag in cells transfected with TRPC5 or TRPC7. In addition to reduction in cell responsiveness, we found that transfection with TRPC1 or TRPC3 shRNA prolongs the lag time from Ag addition to the onset of the $Ca^{2+}$ response compared to cells transfected with TRPC5, TRPC7, or the control shRNA (Fig 6B). These results suggest that TRPC1 and TRPC3 play a significant role in the initiating $Ca^{2+}$ wave phase of the cellular response to Ag stimulation.

Most notably, expression of TRPC1 and TRPC3 shRNA results in decreased frequency of $Ca^{2+}$ wave initiation from cell protrusions compared to expression of mock shRNA (Figure 6C). Expression of TRPC7 shRNA also decreases the frequency of $Ca^{2+}$ wave initiation from cell protrusions, even though this construct does not significantly alter the capacity of the cells to respond or the lag time of the response. Measurements of $Ca^{2+}$ wave velocity show only marginal differences for cells expressing the TRPC shRNA constructs, suggesting that these channels are not involved in $Ca^{2+}$ wave propagation (data not shown). These results also indicate that reduction in the capacity of cells to respond to Ag stimulation after the TRPC1 or TRPC3 shRNA expression is caused by perturbation of wave initiation of the $Ca^{2+}$ response, rather than in later steps involved in propagating the $Ca^{2+}$ signal, which have been shown to be inhibited by TRPC5 shRNA (25).

## DISCUSSION

IgE receptor-mediated $Ca^{2+}$ mobilization plays key roles in mast cell activation and consequent exocytotic release of inflammation and allergy-related mediators. Previous studies characterized dramatic $Ca^{2+}$ oscillations stimulated by Ag in these cells (15) that correlate temporally to exocytotic events (13,15). In the present study we used high-speed confocal imaging to characterize rapid, early events in stimulated $Ca^{2+}$ mobilization with high spatial resolution. Our principal new finding is that the initial increase in cytoplasmic $Ca^{2+}$ in response to Ag stimulation in RBL mast cells is highly spatially organized, initiating at specific regions of the cell and propagating through the cytosol as a $Ca^{2+}$ wave. The existence and nature of $Ca^{2+}$ waves in hematopoietic cells has been controversial, and the study characterizing high-speed, circumferential waves in neutrophils (63) could not be confirmed (64). Lee and Oliver previously described evidence for a $Ca^{2+}$ influx pathway in RBL cells that precedes $Ca^{2+}$ release from intracellular stores (65). The $Ca^{2+}$ waves stimulated via FcεRI that we have characterized in the present study are similar in several aspects to $Ca^{2+}$ waves observed in certain excitable and other non-hematopoietic cells (6,7,66), but they have not been previously detected in Ca responses stimulated by multichain immune recognition receptors.

In certain cell types, elementary $Ca^{2+}$ events such as $Ca^{2+}$ puffs can lead to initiation and propagation of a $Ca^{2+}$ wave, and this has been shown to be regulated by a number of factors, including spatial organization of intracellular $Ca^{2+}$ release sites (67-70). In RBL mast cells, the high incidence of wave initiation from elongated cellular protrusions suggests that these protrusions contain specialized structures that ignite the cellular response. Interestingly, the percentage of stimulated $Ca^{2+}$ waves that initiate from protrusions increases at weak stimulation indicating that protrusions are particularly sensitive to Ag. A survey of the literature indicates that such protrusions are a common feature of mucosal mast cells in tissue sites (34,36,37,71), consistent with an important role for these protrusions in mast cell physiology. The high sensitivity of wave initiation in protrusions that we observe could result from locally enhanced coupling of the IgE receptor and the machinery responsible for $Ca^{2+}$ release from stores. We do not detect enhanced expression of FcεRI in these protrusions, but we find that initiation of $Ca^{2+}$ waves in protrusions is selectively reduced in the absence of extracellular $Ca^{2+}$, suggesting a facilitating $Ca^{2+}$ influx pathway at these protrusions. As discussed below, our results point to $Ca^{2+}$- dependent potentiation of $IP_3$ receptors close to sites of $Ca^{2+}$ influx at protrusions, rendering these receptors more sensitive and therefore more probable sites for $Ca^{2+}$ wave initiation.

$Ca^{2+}$ oscillations following initial waves exhibit a global, non-directional increase in $Ca^{2+}$ concentration that contrasts with directional $Ca^{2+}$ elevation seen for the waves. Because of this spatial distinction and the pharmacological differences, we conclude that waves and oscillations are two discrete but coupled $Ca^{2+}$ events in IgE receptor-mediated signaling. We

suggest that $Ca^{2+}$ waves are the initiating event of mast cell activation, established by the unique spatial distribution of $Ca^{2+}$ influx pathways in these cells, involving TRPC channels that may be preferentially expressed in the elongated protrusions, rendering these to be more sensitive to Ag stimulation. Subsequent to the waves are $Ca^{2+}$ oscillations that are thought to result from $IP_3$-induced release of $Ca^{2+}$ from ER (72). These reoccurring $Ca^{2+}$ elevations were suggested to play a role in prolonging the duration of the $Ca^{2+}$ signal, enhancing its efficacy (16) and also in providing temporal encoding for downstream events such as degranulation (15). Interestingly, we could occasionally detect $Ca^{2+}$ oscillations in cells that did not demonstrate a $Ca^{2+}$ wave upon Ag stimulation, suggesting that the propagation of $Ca^{2+}$ through the cytoplasm during the wave period is not required for the onset of $Ca^{2+}$ oscillations.

In addition to $Ca^{2+}$ waves and oscillations, we detect $Ca^{2+}$ puffs in cells stimulated by antigen under certain conditions. Of particular interest are the repetitive $Ca^{2+}$ puffs that are elicited by local application of antigen with a DNP-BSA coated micropipette, demonstrating that the molecular machinery capable of initiating local $Ca^{2+}$ responses is distributed throughout the cell and is not restricted to the protrusions. $Ca^{2+}$ puffs stimulated by Ag-coated micropipette contact are similarly frequent in the absence of extracellular $Ca^{2+}$, indicating that the generation of spatially restricted $Ca^{2+}$ elevations in these cells involves $Ca^{2+}$ release from stores and does not require $Ca^{2+}$ influx. However, the periodic nature of these puffs suggests a complex mechanism for their regulation that may be related to the periodic nature of more global $Ca^{2+}$ oscillations elicited by soluble antigen. It will be interesting to determine whether these localized $Ca^{2+}$ puffs are sufficient to elicit localize exocytosis in these cells.

Pharmacologic characterization of IgE receptor-mediated $Ca^{2+}$ waves yield evidence for PLC activation in this mechanism, whereas store-operated $Ca^{2+}$ entry does not appear to play an important role in this early phase of the $Ca^{2+}$ response. PLCγ-dependent $IP_3$ production is important for generating $Ca^{2+}$ responses to Ag in mast cells (73), and it is possible that a specific $IP_3$ receptor family member is involved in $Ca^{2+}$ wave initiation. The greater sensitivity of $IP_3R$-3 to $Ca^{2+}$ release by $IP_3$ (74) suggests this family member as a strong candidate for initiation of an $IP_3$-dependent $Ca^{2+}$ wave at protrusions. $Ca^{2+}$ waves can be triggered by alternate means of $Ca^{2+}$ mobilization, including $Ca^{2+}$ ionophore and thapsigargin, but these agents cause less frequent $Ca^{2+}$ waves (Table I). Furthermore, initiation of $Ca^{2+}$ waves by $Ca^{2+}$ ionophore occurs only infrequently at extended protrusions. Together, these results suggest that $Ca^{2+}$ responses initiated by the IgE receptor are more spatially regulated than those caused by non-receptor-mediated cell activation.

The recent study by Ma et al. provided evidence that TRPC channels contribute to stimulated $Ca^{2+}$ influx in RBL cells (25), suggesting their possible involvement in the Ag-stimulated $Ca^{2+}$ influx pathway that initiates $Ca^{2+}$ waves from extended protrusions. Our results with shRNA-mediated knockdown of TRPC proteins provide evidence that decreased expression of TRPC1, and, to lesser extent, TRPC3, reduces the responsiveness of these cells to low concentration of Ag (Figure 6A, B) and decreases the frequency of wave initiation from extended protrusions (Figure 6C). At higher concentrations of Ag, TRPC 1 channel knock down is less effective in decreasing the responsiveness of the cells (data not shown), indicating that this channel plays an important role in $Ca^{2+}$ responses only under more physiological conditions of IgE receptor stimulation. Other TRPC channels may also contribute to $Ca^{2+}$ wave initiation, and our failure to detect significant effects of TRPC5 knock down, or the smaller effects of TRPC3 and 7 knock down, may be limited by the efficiency of their reduction under our experimental conditions.

These results suggest that $Ca^{2+}$ influx via TRPC channels, particularly TRPC1, is likely to participate in the initial steps of mast cell activation by enhancing the sensitivity of these cells to threshold Ag stimulation. Although the mechanism for this enhancement is not yet understood, it is likely that a $Ca^{2+}$ influx-dependent increase in $IP_3R$ activation is involved. Two possible mechanisms are indicated in Figure 4D: In one, local accumulation of TRPC at protrusions could enhance receptor-stimulated influx at this region; Alternatively, enhanced physical coupling of the TRPC channels to $IP_3R$ (75), PLCγ (76), or FcεRI in this region could mediate local $Ca^{2+}$ influx to initiate wave propagation.

Our observations that rat BMMCs exhibits similar morphologies as RBL mast cells and initiate $Ca^{2+}$ responses to antigen in the form of waves that begin in extended protrusions show that these stimulated waves are a general feature of FcεRI-mediated $Ca^{2+}$ signaling. Both rat BMMCs (23) and RBL mast cells (20) have marker characteristics of mucosal mast cells, and it is not yet clear whether this wave response is a specific feature of this subset of mast cells. Mouse BMMCs undergo chemotatic responses on vitronectin (77), and it may be possible to observe stimulated $Ca^{2+}$ waves under these conditions of cell attachment.

Our data establish $Ca^{2+}$ waves originating from a specific cellular site as a common feature of the $Ca^{2+}$ response to antigen in RBL mast cells and rat BMMCs, but the physiological function of these waves and the molecular basis for their site of initiation are not completely understood. Regulated $Ca^{2+}$ signaling across the cell is a fundamental mechanism for information transfer between organelles or cellular regions that conveys directional and temporal information**.** In this regard, we have preliminary evidence that direction of RBL cell migration correlates with the site of Ag-stimulated wave initiation (R. Cohen and J. Lee, unpublished results), suggesting a strategic localization of the $Ca^{2+}$ signaling machinery to communicate directional information in these cells. Localized degranulation from extended protrusions might also be mediated by this machinery under certain physiological conditions.

In summary, we show that the response of RBL and rat BMMC to Ag stimulation initiates with a propagating $Ca^{2+}$ wave, most often beginning at the tips of cellular protrusions in a $Ca^{2+}$ influx-dependent manner. These waves initiate with TRPC1-dependent $Ca^{2+}$ influx, then propagate by $Ca^{2+}$-dependent $Ca^{2+}$ release from stores, followed by extracellular $Ca^{2+}$-dependent oscillations. Spatial localization of wave initiation sites to extended protrusions suggests a link between this signaling response and polarized cell motility. Our results indicate that when mast cells encounter physiological levels of antigen that are insufficient to directly activate global $Ca^{2+}$ mobilization, activation of $Ca^{2+}$ influx mediated by TRPC1 channels in extended cell protrusions can ignite a response that is propagated and amplified. In this manner, the initiation of a physiological cellular response is both spatially and temporally controlled.

## Supplementary Material

Refer to Web version on PubMed Central for supplementary material.

## Acknowledgments

We thank Robert Doran for excellent technical support and Dr. Michael Kotlikoff for the GCaMP2 construct and valuable discussions. We are grateful to Lisa Blum from the laboratory of Dr. Judith Appleton and Norah Smith and Jinmin Lee for preparation and culture of rat BMMCs**.** We also thank Dr. Clare Fewtrell for helpful comments on the manuscript and Dr. Reuben Siraganian for purified mAb AA4.

This work was supported by NIH Grant AI022449 and by the Nanobiotechnology Center at Cornell (NSF:ECS-9876771). H-T Ma is supported by the International Program of NHLBI, NIH.

## REFERENCES


1. Clapham DE. Calcium signaling. Cell 2007;131:1047–58. [PubMed: 18083096]
2. Berridge MJ. Calcium signal transduction and cellular control mechanisms. Biochim Biophys Acta 2004;1742:3–7. [PubMed: 15590051]
3. Berridge MJ. Calcium microdomains: organization and function. Cell Calcium 2006;40:405–412. [PubMed: 17030366]
4. Ridgway EB, Gilkey JC, Jaffe LF. Free calcium increases explosively in activating medaka eggs. Proc Natl Acad Sci U S A 1977;74:623–627. [PubMed: 322135]
5. Jaffe L. On the conservation of fast calcium wave speeds. Cell Calcium 2002;32:217–229. [PubMed: 12379182]
6. Robb-Gaspers LD, Thomas AP. Coordination of Ca2+ signaling by intercellular propagation of Ca2+ waves in the intact liver. J Biol Chem 1995;270:8102–8107. [PubMed: 7713913]
7. Rintoul GL, Baimbridge KG. Effects of calcium buffers and calbindin-D28k upon histamine-induced calcium oscillations and calcium waves in HeLa cells. Cell Calcium 2003;34:131–144. [PubMed: 12810055]
8. Hillson EJ, Hallett MB. Localised and rapid Ca2+ micro-events in human neutrophils: conventional Ca2+ puffs and global waves without peripheral-restriction or wave cycling. Cell Calcium 2007;41:525–536. [PubMed: 17324458]
9. Mackenzie L, Bootman MD, Berridge MJ, Lipp P. Predetermined recruitment of calcium release sites underlies excitation-contraction coupling in rat atrial myocytes. J Physiol 2001;530:417–429. [PubMed: 11158273]
10. Jaffe LF. The path of calcium in cytosolic calcium oscillations: a unifying hypothesis. Proc Natl Acad Sci U S A 1991;88:9883–9887. [PubMed: 1946414]
11. Thomas AP, Bird GS, Hajnoczky G, Robb-Gaspers LD, Putney JW Jr. Spatial and temporal aspects of cellular calcium signaling. FASEB J 1996;10:1505–1517. [PubMed: 8940296]
12. Tovey SC, de Smet P, Lipp P, Thomas D, Young KW, Missiaen L, De Smedt H, Parys JB, Berridge MJ, Thuring J, Holmes A, Bootman MD. Calcium puffs are generic InsP(3)-activated elementary calcium signals and are downregulated by prolonged hormonal stimulation to inhibit cellular calcium responses. J Cell Sci 2001;114:3979–3989. [PubMed: 11739630]
13. Millard PJ, Gross D, Webb WW, Fewtrell C. Imaging asynchronous changes in intracellular Ca2+ in individual stimulated tumor mast cells. Proc Natl Acad Sci U S A 1988;85:1854–1858. [PubMed: 3162312]
14. Ryan TA, Millard PJ, Webb WW. Imaging [Ca2+]i dynamics during signal transduction. Cell Calcium 1990;11:145–155. [PubMed: 2141302]
15. Kim TD, Eddlestone GT, Mahmoud SF, Kuchtey J, Fewtrell C. Correlating Ca2+ responses and secretion in individual RBL-2H3 mucosal mast cells. J Biol Chem 1997;272:31225–31229. [PubMed: 9395446]
16. Narenjkar J, Marsh SJ, Assem ES. The characterization and quantification of antigen-induced Ca2+ oscillations in a rat basophilic leukaemia cell line (RBL-2H3). Cell Calcium 1999;26:261–269. [PubMed: 10668564]
17. Parekh AB. Functional consequences of activating store-operated CRAC channels. Cell Calcium 2007;42:111–121. [PubMed: 17445883]
18. Galli SJ, Grimbaldeston M, Tsai M. Immunomodulatory mast cells: negative, as well as positive, regulators of immunity. Nat Rev Immunol 2008;8:478–486. [PubMed: 18483499]
19. Rivera J, Gilfillan AM. Molecular regulation of mast cell activation. J Allergy Clin Immunol 2006;117:1214–1225. quiz 1226. [PubMed: 16750977]
20. Seldin DC, Adelman S, Austen KF, Stevens RL, Hein A, Caulfield JP, Woodbury RG. Homology of the rat basophilic leukemia cell and the rat mucosal mast cell. Proc Natl Acad Sci U S A 1985;82:3871–3875. [PubMed: 3923482]
21. Wong GW, Tang Y, Feyfant E, Sali A, Li L, Li Y, Huang C, Friend DS, Krilis SA, Stevens RL. Identification of a new member of the tryptase family of mouse and human mast cell proteases which possesses a novel COOH-terminal hydrophobic extension. J Biol Chem 1999;274:30784–30793. [PubMed: 10521469]

22. Razin E, Zhang ZC, Nechushtan H, Frenkel S, Lee YN, Arudchandran R, Rivera J. Suppression of microphthalmia transcriptional activity by its association with protein kinase C-interacting protein 1 in mast cells. J Biol Chem 1999;274:34272–34276. [PubMed: 10567402]
23. MacDonald AJ, Pick J, Bissonnette EY, Befus AD. Rat mucosal mast cells: the cultured bone marrow-derived mast cell is biochemically and functionally analogous to its counterpart in vivo. Immunology 1998;93:533–539. [PubMed: 9659226]
24. Tallini YN, Ohkura M, Choi BR, Ji G, Imoto K, Doran R, Lee J, Plan P, Wilson J, Xin HB, Sanbe A, Gulick J, Mathai J, Robbins J, Salama G, Nakai J, Kotlikoff MI. Imaging cellular signals in the heart in vivo: Cardiac expression of the high-signal Ca2+ indicator GCaMP2. Proc Natl Acad Sci U S A 2006;103:4753–4758. [PubMed: 16537386]
25. Ma HT, Peng Z, Hiragun T, Iwaki S, Gilfillan AM, Beaven MA. Canonical transient receptor potential 5 channel in conjunction with Orai1 and STIM1 allows Sr2+ entry, optimal influx of Ca2+, and degranulation in a rat mast cell line. J Immunol 2008;180:2233–2239. [PubMed: 18250430]
26. Barsumian EL, Isersky C, Petrino MG, Siraganian RP. IgE-induced histamine release from rat basophilic leukemia cell lines: isolation of releasing and nonreleasing clones. Eur J Immunol 1981;11:317–323. [PubMed: 6166481]
27. Haig DM, Huntley JF, MacKellar A, Newlands GF, Inglis L, Sangha R, Cohen D, Hapel A, Galli SJ, Miller HR. Effects of stem cell factor (kit-ligand) and interleukin-3 on the growth and serine proteinase expression of rat bone-marrow-derived or serosal mast cells. Blood 1994;83:72–83. [PubMed: 7506083]
28. Posner RG, Lee B, Conrad DH, Holowka D, Baird B, Goldstein B. Aggregation of IgE-receptor complexes on rat basophilic leukemia cells does not change the intrinsic affinity but can alter the kinetics of the ligand-IgE interaction. Biochemistry 1992;31:5350–5356. [PubMed: 1534998]
29. Gosse JA, Wagenknecht-Wiesner A, Holowka D, Baird B. Transmembrane sequences are determinants of immunoreceptor signaling. J Immunol 2005;175:2123–2131. [PubMed: 16081778]
30. Guo NH, Her GR, Reinhold VN, Brennan MJ, Siraganian RP, Ginsburg V. Monoclonal antibody AA4, which inhibits binding of IgE to high affinity receptors on rat basophilic leukemia cells, binds to novel alpha-galactosyl derivatives of ganglioside GD1b. J Biol Chem 1989;264:13267–13272. [PubMed: 2526814]
31. Pierini L, Holowka D, Baird B. Fc epsilon RI-mediated association of 6-micron beads with RBL-2H3 mast cells results in exclusion of signaling proteins from the forming phagosome and abrogation of normal downstream signaling. J Cell Biol 1996;134:1427–1439. [PubMed: 8830772]
32. Torres AJ, Vasudevan L, Holowka D, Baird BA. Focal adhesion proteins connect IgE receptors to the cytoskeleton as revealed by micropatterned ligand arrays. Proc Natl Acad Sci U S A 2008;105:17238–17244. [PubMed: 19004813]
33. Kotlikoff MI. Genetically encoded Ca2+ indicators: using genetics and molecular design to understand complex physiology. J Physiol 2007;578:55–67. [PubMed: 17038427]
34. Metcalfe DD, Baram D, Mekori YA. Mast cells. Physiol Rev 1997;77:1033–1079. [PubMed: 9354811]
35. Crivellato E, Baldini G, Basa M, Fusaroli P. The three-dimensional structure of interdigitating cells. Ital J Anat Embryol 1993;98:243–258. [PubMed: 8018016]
36. Demitsu T, Kiyosawa T, Kakurai M, Murata S, Yaoita H. Local injection of recombinant human stem cell factor promotes human skin mast cell survival and neurofibroma cell proliferation in the transplanted neurofibroma in nude mice. Arch Dermatol Res 1999;291:318–324. [PubMed: 10421057]
37. Shaikh N, Rivera J, Hewlett BR, Stead RH, Zhu FG, Marshall JS. Mast cell Fc epsilonRI expression in the rat intestinal mucosa and tongue is enhanced during Nippostrongylus brasiliensis infection and can be up-regulated by in vivo administration of IgE. J Immunol 1997;158:3805–3812. [PubMed: 9103447]
38. Kwan CY, Putney JW Jr. Uptake and intracellular sequestration of divalent cations in resting and methacholine-stimulated mouse lacrimal acinar cells. Dissociation by Sr2+ and Ba2+ of agonist-

stimulated divalent cation entry from the refilling of the agonist-sensitive intracellular pool. J Biol Chem 1990;265:678–684. [PubMed: 2404009]

39. Bootman MD, Berridge MJ, Lipp P. Cooking with calcium: the recipes for composing global signals from elementary events. Cell 1997;91:367–373. [PubMed: 9363945]
40. Hoth M, Penner R. Depletion of intracellular calcium stores activates a calcium current in mast cells. Nature 1992;355:353–356. [PubMed: 1309940]
41. Bakowski D, Parekh AB. Voltage-dependent Ba2+ permeation through store-operated CRAC channels: implications for channel selectivity. Cell Calcium 2007;42:333–339. [PubMed: 17343911]
42. Basciano LK, Berenstein EH, Kmak L, Siraganian RP. Monoclonal antibodies that inhibit IgE binding. J Biol Chem 1986;261:11823–11831. [PubMed: 2943732]
43. Jamur MC, Grodzki AC, Berenstein EH, Hamawy MM, Siraganian RP, Oliver C. Identification and characterization of undifferentiated mast cells in mouse bone marrow. Blood 2005;105:4282–4289. [PubMed: 15718418]
44. Enerback L. Mast cells in rat gastrointestinal mucosa. 2 Dye-binding and metachromatic properties. Acta Pathol Microbiol Scand 1966;66:303–312. [PubMed: 4162018]
45. Parker I, Yao Y. Regenerative release of calcium from functionally discrete subcellular stores by inositol trisphosphate. Proc Biol Sci 1991;246:269–274. [PubMed: 1686093]
46. Yao Y, Choi J, Parker I. Quantal puffs of intracellular Ca2+ evoked by inositol trisphosphate in Xenopus oocytes. J Physiol 1995;482(Pt 3):533–553. [PubMed: 7738847]
47. Taylor CW, Broad LM. Pharmacological analysis of intracellular Ca2+ signalling: problems and pitfalls. Trends Pharmacol Sci 1998;19:370–375. [PubMed: 9786025]
48. Lee HS, Park CS, Lee YM, Suk HY, Clemons TC, Choi OH. Antigen-induced Ca2+ mobilization in RBL-2H3 cells: role of I(1,4,5)P3 and S1P and necessity of I(1,4,5)P3 production. Cell Calcium 2005;38:581–592. [PubMed: 16219349]
49. Maruyama T, Kanaji T, Nakade S, Kanno T, Mikoshiba K. 2APB, 2-aminoethoxydiphenyl borate, a membrane-penetrable modulator of Ins(1,4,5)P3-induced Ca2+ release. J Biochem 1997;122:498–505. [PubMed: 9348075]
50. Prakriya M, Lewis RS. Potentiation and inhibition of Ca(2+) release-activated Ca(2+) channels by 2-aminoethyldiphenyl borate (2-APB) occurs independently of IP(3) receptors. J Physiol 2001;536:3–19. [PubMed: 11579153]
51. Bakowski D, Glitsch MD, Parekh AB. An examination of the secretion-like coupling model for the activation of the Ca2+ release-activated Ca2+ current I(CRAC) in RBL-1 cells. J Physiol 2001;532:55–71. [PubMed: 11283225]
52. Iwasaki H, Mori Y, Hara Y, Uchida K, Zhou H, Mikoshiba K. 2-Aminoethoxydiphenyl borate (2-APB) inhibits capacitative calcium entry independently of the function of inositol 1,4,5-trisphosphate receptors. Receptors Channels 2001;7:429–439. [PubMed: 11918346]
53. Broad LM, Braun FJ, Lievremont JP, Bird GS, Kurosaki T, Putney JW Jr. Role of the phospholipase C-inositol 1,4,5-trisphosphate pathway in calcium release-activated calcium current and capacitative calcium entry. J Biol Chem 2001;276:15945–15952. [PubMed: 11278938]
54. Mathes C, Fleig A, Penner R. Calcium release-activated calcium current (ICRAC) is a direct target for sphingosine. J Biol Chem 1998;273:25020–25030. [PubMed: 9737958]
55. Itagaki K, Hauser CJ. Sphingosine 1-phosphate, a diffusible calcium influx factor mediating store-operated calcium entry. J Biol Chem 2003;278:27540–27547. [PubMed: 12746430]
56. Jolly PS, Bektas M, Olivera A, Gonzalez-Espinosa C, Proia RL, Rivera J, Milstien S, Spiegel S. Transactivation of sphingosine-1-phosphate receptors by FcepsilonRI triggering is required for normal mast cell degranulation and chemotaxis. J Exp Med 2004;199:959–970. [PubMed: 15067032]
57. Calloway N, Vig M, Kinet JP, Holowka D, Baird B. Molecular clustering of STIM1 with Orai1/CRACM1 at the plasma membrane depends dynamically on depletion of Ca2+ stores and on electrostatic interactions. Mol Biol Cell 2009;20:389–399. [PubMed: 18987344]
58. Suzuki Y, Yoshimaru T, Inoue T, Nunomura S, Ra C. The high-affinity immunoglobulin E receptor (FcepsilonRI) regulates mitochondrial calcium uptake and a dihydropyridine receptor-

mediated calcium influx in mast cells: Role of the FcepsilonRIbeta chain immunoreceptor tyrosine-based activation motif. Biochem Pharmacol 2008;75:1492–1503. [PubMed: 18243160]

59. Lin X, Hume RI, Nuttall AL. Dihydropyridines and verapamil inhibit voltage-dependent K+ current in isolated outer hair cells of the guinea pig. Hear Res 1995;88:36–46. [PubMed: 8576001]
60. Jensen BS, Strobaek D, Christophersen P, Jorgensen TD, Hansen C, Silahtaroglu A, Olesen SP, Ahring PK. Characterization of the cloned human intermediate-conductance Ca2+-activated K+ channel. Am J Physiol 1998;275:C848–856. [PubMed: 9730970]
61. Dellis O, Dedos SG, Tovey SC, Taufiq Ur R, Dubel SJ, Taylor CW. Ca2+ entry through plasma membrane IP3 receptors. Science 2006;313:229–233. [PubMed: 16840702]
62. Pizzo P, Burgo A, Pozzan T, Fasolato C. Role of capacitative calcium entry on glutamate-induced calcium influx in type-I rat cortical astrocytes. J Neurochem 2001;79:98–109. [PubMed: 11595762]
63. Kindzelskii AL, Petty HR. Intracellular calcium waves accompany neutrophil polarization, formylmethionylleucylphenylalanine stimulation, and phagocytosis: a high speed microscopy study. J Immunol 2003;170:64–72. [PubMed: 12496384]
64. Petty HR. Letter of retraction. J Immunol 2009;182:1770. [PubMed: 19155527]
65. Lee RJ, Oliver JM. Roles for Ca2+ stores release and two Ca2+ influx pathways in the Fc epsilon R1-activated Ca2+ responses of RBL-2H3 mast cells. Mol Biol Cell 1995;6:825–839. [PubMed: 7579697]
66. Nagata J, Guerra MT, Shugrue CA, Gomes DA, Nagata N, Nathanson MH. Lipid rafts establish calcium waves in hepatocytes. Gastroenterology 2007;133:256–267. [PubMed: 17631147]
67. Berridge MJ. Elementary and global aspects of calcium signalling. J Physiol 1997;499(Pt 2):291–306. [PubMed: 9080360]
68. Marchant J, Callamaras N, Parker I. Initiation of IP(3)-mediated Ca(2+) waves in Xenopus oocytes. EMBO J 1999;18:5285–5299. [PubMed: 10508162]
69. Marchant JS, Parker I. Role of elementary Ca(2+) puffs in generating repetitive Ca(2+) oscillations. EMBO J 2001;20:65–76. [PubMed: 11226156]
70. Bootman MD, Lipp P, Berridge MJ. The organisation and functions of local Ca(2+) signals. J Cell Sci 2001;114:2213–2222. [PubMed: 11493661]
71. Crivellato E, Finato N, Isola M, Ribatti D, Beltrami CA. Low mast cell density in the human duodenal mucosa from chronic inflammatory duodenal bowel disorders is associated with defective villous architecture. Eur J Clin Invest 2003;33:601–610. [PubMed: 12814398]
72. Ma HT, Beaven MA. Regulation of Ca2+ signaling with particular focus on mast cells. Crit Rev Immunol 2009;29:155–186. [PubMed: 19496745]
73. Wen R, Jou ST, Chen Y, Hoffmeyer A, Wang D. Phospholipase C gamma 2 is essential for specific functions of Fc epsilon R and Fc gamma R. J Immunol 2002;169:6743–6752. [PubMed: 12471105]
74. Thrower EC, Hagar RE, Ehrlich BE. Regulation of Ins(1,4,5)P3 receptor isoforms by endogenous modulators. Trends Pharmacol Sci 2001;22:580–586. [PubMed: 11698102]
75. Kiselyov K, Mignery GA, Zhu MX, Muallem S. The N-terminal domain of the IP3 receptor gates store-operated hTrp3 channels. Mol Cell 1999;4:423–429. [PubMed: 10518223]
76. van Rossum DB, Patterson RL, Sharma S, Barrow RK, Kornberg M, Gill DL, Snyder SH. Phospholipase Cgamma1 controls surface expression of TRPC3 through an intermolecular PH domain. Nature 2005;434:99–104. [PubMed: 15744307]
77. Taub D, Dastych J, Inamura N, Upton J, Kelvin D, Metcalfe D, Oppenheim J. Bone marrow-derived murine mast cells migrate, but do not degranulate, in response to chemokines. J Immunol 1995;154:2393–2402. [PubMed: 7532669]

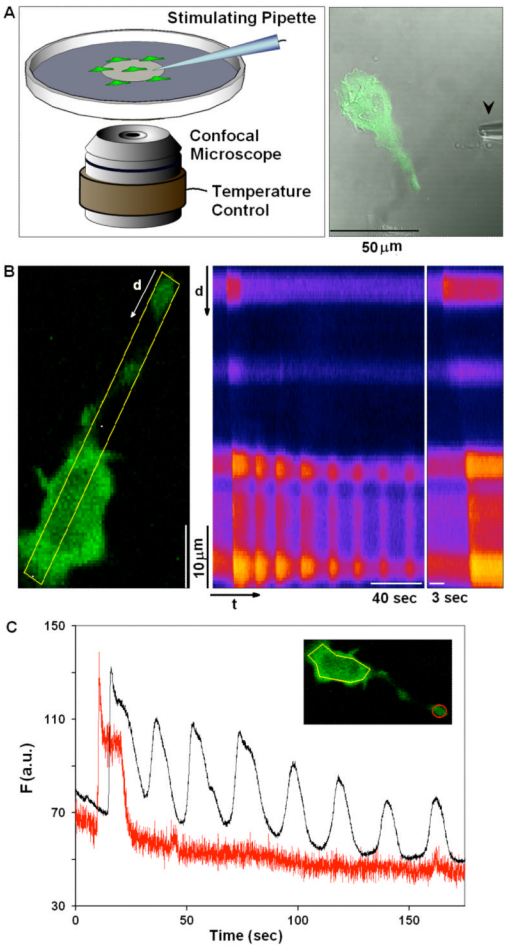


**Figure 1. Visualization of $Ca^{2+}$ dynamics in individual RBL mast cells**

A) Cells were plated at low density on MatTek dishes, and individual cells were stimulated using a pulled capillary (arrow; 0.5-1 μm diameter), filled with stimulating solution (as specified for each experiment) that was puffed at the cell (5psi/10sec pulse) from a distance within 100 μm. B) Image of RBL cell expressing GCaMP2 and sensitized with anti-DNP IgE, stimulated with a puff of 1.7 μg/ml Ag (DNP-BSA). Middle panel shows time line analysis of the stimulated cell and changes in $Ca^{2+}$ concentration occurring over time in the 7 pixel wide line segment defined in the left panel. Changes in $Ca^{2+}$ concentration are indicated by relative changes in brightness, where brighter colors represent higher $Ca^{2+}$ concentration. Right panel expands early time points of the time line analysis and highlights our general observation that $Ca^{2+}$ elevation initiates in cellular protrusions and propagates through the cell body. C) Traces of GCaMP2 intensity changes over time as calculated for the same cell imaged in B (inset). Black and red traces represent the changes in $Ca^{2+}$ concentration in cell body (yellow ROI) or cell protrusion (red ROI), respectively.

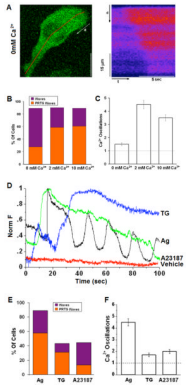


**Figure 2. Dependence of stimulated $Ca^{2+}$ waves and oscillations on extracellular $Ca^{2+}$and stimulus**

A) Representative cell sensitized with IgE and stimulated with 1.7μg/ml Ag in the absence of extracellular $Ca^{2+}$. Right panel shows time line analysis for early time points and indicated segment in left panel image. B) Histogram showing percentage of cells responding to stimulus with $Ca^{2+}$ waves as averaged over multiple experiments for 0mM $Ca^{2+}$ (n=29), 2mM $Ca^{2+}$ (n=80); 10mM $Ca^{2+}$ (n=28). Bar height shows total percentage of waves; orange portion represents the percentage of waves originating in protrusions (PRTS). C) Average number of oscillations within 2 min of stimulation under specified conditions. D) Representative traces of cells sensitized with anti-DNP IgE and stimulated with puff from pipette containing 1.7 μg/ml DNP-BSA (Ag), 1μM thapsigargin (TG), 20μM A23187 or BSS buffer only (vehicle). E) Percentage of cells responding to stimulus with $Ca^{2+}$ waves averaged over multiple experiments and represented as in (B) with indicated conditions: Ag (n=80); TG (n=16); A23187 (n=29). F) Average number of oscillations within 2 min of stimulation under specified conditions. The first oscillation corresponds to the originating $Ca^{2+}$ wave (dotted line). Error bars correspond to standard error of the mean (SEM).

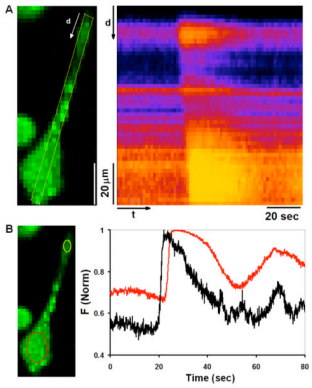


**Figure 3. $Ca^{2+}$ dynamics in individual rat BMMCs**

A) Confocal image of a representative rat BMMC sensitized with anti-DNP IgE and loaded with Fluo5F (left panel), and time line analysis of indicated ROI for this cell stimulated at t=0 with a puff of 1.7 μg/ml DNP-BSA (right panel). Changes in $Ca^{2+}$ concentration in response to stimulation are depicted, where brighter colors represent higher $Ca^{2+}$ concentration. Time line analysis highlights the $Ca^{2+}$ elevation initiating in the tip of the cellular protrusion and propagating through the cell body. B) Traces of Fluo5F intensity changes over time as calculated for the same cell imaged in (A). Black and red traces in right panel represent changes in $Ca^{2+}$ concentration in cell body (yellow ROI) and in cell protrusion (red ROI), respectively, in the left panel.

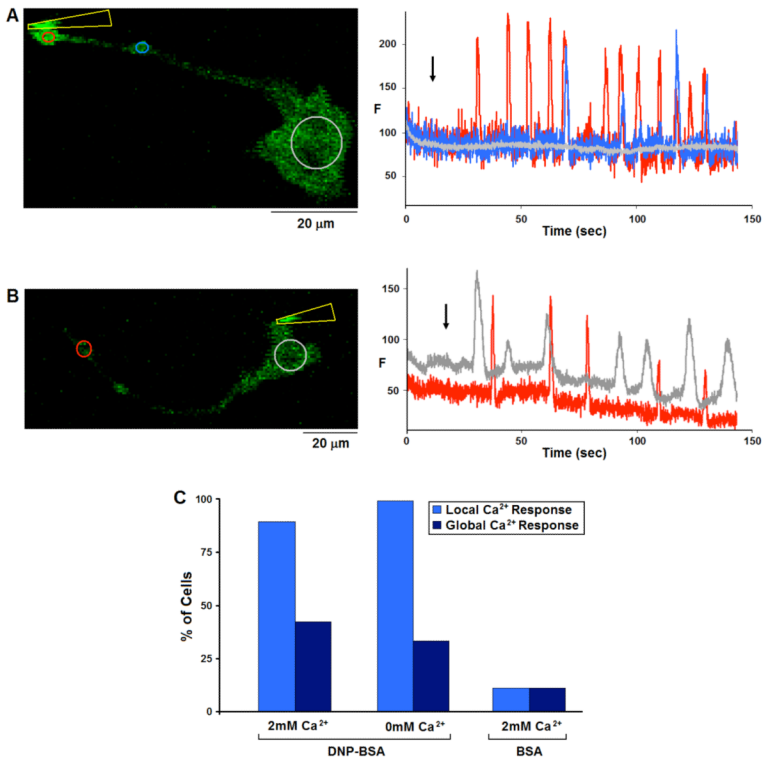


**Figure 4. Stimulation of RBL cells by contact with Ag-coated micropipette**

A and B) Representative cells expressing GCaMP2, sensitized with IgE and stimulated with DNP-BSA conjugated micropipettes. A) Micropipette (indicated by yellow arrowhead) contacting the cell at the tip of a protrusion elicits a train of spatially restricted $Ca^{2+}$ puffs, each traveling no more than 30μm along the protrusion. B) Contact stimulation at the cell body results repetitive $Ca^{2+}$ puffs in the cell body that sometimes propagate as a wave to the protrusion. Left panels show images with ROIs defined; Right panels show $Ca^{2+}$ concentration changes in ROIs of corresponding color. Black arrow indicates initiation of contact between micropipette and cell. C) Histogram showing percentage of cells responding with local $Ca^{2+}$ puffs only (light blue) or more global $Ca^{2+}$ elevation (dark blue) due to contact with DNP-BSA-conjugated micropipettes in the presence (n=28) or absence (n=18) of extracellular $Ca^{2+}$, or with unmodified BSA-conjugated micropipettes (n=18).

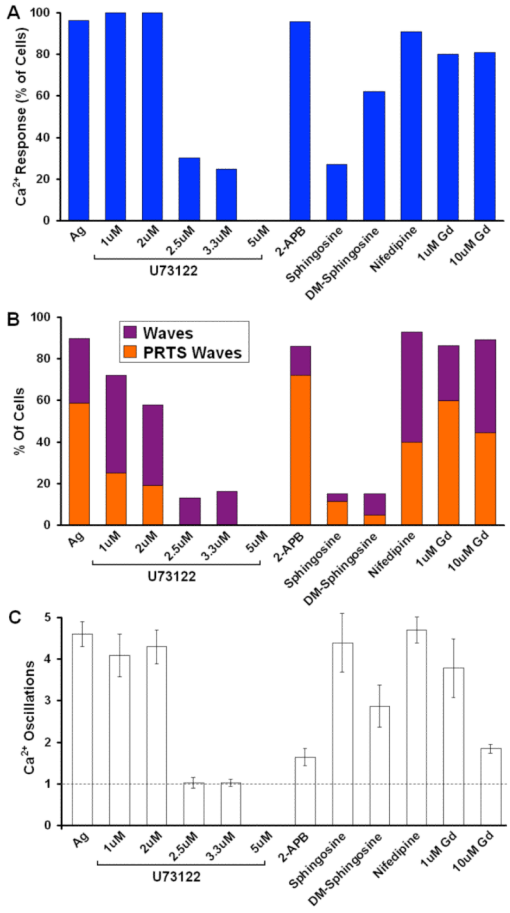


**Figure 5. Effects of inhibitors on intracellular $Ca^{2+}$ waves and oscillations**

A) Percentage of cells from multiple experiments showing a measurable $Ca^{2+}$ response to stimulation by 1.7 μg/ml Ag in the presence of the following reagents in the extracellular buffer: 1-5 μM U73122 (n>18 each), 20mM 2-APB (n=23), 8μM D-sphingosine (n=26); 8μM DM-sphingosine (n=31), 10μM nifedipine (n=15), 1 or 10 μM $GdCl_3$ ($Gd^{3+}$; n>20 each) B) Percentage of cells responding to stimulus with $Ca^{2+}$ waves as averaged over multiple experiments with indicated conditions. Bar height shows total % waves; orange portion represents % waves originating in protrusions. C) Average number of oscillations within 2 min of stimulation under specified conditions. The first oscillation corresponds to the originating $Ca^{2+}$ wave (dotted line). Error bars correspond to SEM.

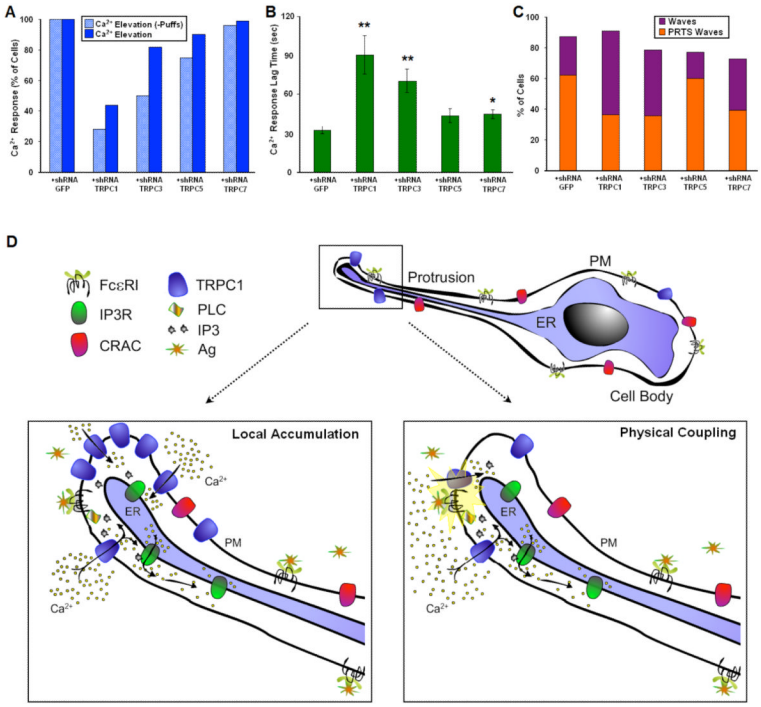


**Figure 6. Participation of TRPC channels in Ag stimulated initiation of the $Ca^{2+}$ response**

RBL cells were co-transfected with GCaMP2 and shRNA plasmids targeting TRPC1, 3, 5, 7 or mock sequence (for each condition n>29). Cells sensitized with anti-DNP IgE were stimulated with puff from pipette containing 1.7 ng/ml DNP-BSA in BSS. A) Percentage of cells from multiple experiments showing a measurable $Ca^{2+}$ response corresponding to elevation of intracellular $Ca^{2+}$ cells. Dark blue bars include cells that only include $Ca^{2+}$ puffs in the count, and light blue bars exclude this population. B) Average lag time before initiation of $Ca^{2+}$ wave with specified shRNA. Error bars correspond to SEM. *P < 0.05, **P < 0.01 vs. cells expressing shGFP. C) Percentage of cells responding to stimulus with $Ca^{2+}$ waves with indicated shRNA. Bar height shows total % waves; orange portion represents % waves originating in protrusions. D) Model for initiation of $Ca^{2+}$ mobilization in extended protrusions. Ag crosslinks IgE/FcεRI complexes, activating $Ca^{2+}$ influx via TRPC1 channels to cause local increase in cytoplasmic $Ca^{2+}$ at the tip of a cell protrusion. This potentiates $IP_3$-mediated $Ca^{2+}$ release from the nearby ER store that propagates via $Ca^{2+}$-induced $Ca^{2+}$ release to generate a $Ca^{2+}$ wave that initiates $Ca^{2+}$ oscillations and cell activation. Two possible mechanisms for wave initiation at these protrusions are indicated.

**Table I**

Summary of $Ca^{2+}$ Response Parameters with GCaMP2[a]

| | Condition | Response (% of Cells) | $Ca^{2+}$ Waves (% of Cells) | Waves from PRTS (% of Waves) | Oscillations[b] | wave velocity (μm/sec) | Laq Time (sec) |
|---|---|---|---|---|---|---|---|
| Ag | 1700ng/ml | 96.3 | 90 | 65 | 4.5 ± 0.3 | 42.6 ± 4 | 19.4 ± 1.25 |
| | 170ng/ml | 94 | 87 | 54 | 4.9 ± 0.4 | 37.3 ± 5.1 | 19.5 ± 2.1 |
| | 17ng/ml | 90.5 | 81 | 62 | 5 ± 0.4 | 18.7 ± 2.2 | 41.8 ± 4.4 |
| | 1.7ng/ml | 53.8 | 78 | 86 | 3.7 ± 0.9 | 15.9 ± 1.6 | 42.6 ± 6.5 |
| | $0[Ca^{2+}]_o$ | 96.8 | 89 | 31 | 1.5 ± 0.1 | 25.8 ± 4.5 | 30.2 ± 4.2 |
| | 50mM KCl | 91 | 73 | 27.2 | 5.7 ± 0.5 | 27.8 ± 4.2 | 30.2 ± 4.9 |
| | 2mM $Ba^{2+}$ | 64 | 78 | 72 | 1.6 ± 0.3 | 46.9 ± 3.5 | 20.9 ± 0.8 |
| | 2mM $Sr^{2+}$ | 90 | 89 | 75 | 1.7 ± 0.2 | 44.4 ± 3.6 | 19.4 ± 1.5 |
| | TG | 76.2 | 43.7 | 71 | 1.7 ± 0.2 | 30.3 ± 16.4 | 29.1 ± 4 |
| | A23187 | 73.9 | 44.8 | 30.7 | 2 ± 0.2 | 19.9 ± 5.3 | 17.9 ± 2.7 |
| | U73122 1μM | 100 | 72 | 35 | 4 ± 0.5 | 47.2 ± 11 | 14.8 ± 2.3 |
| | U73122 2μM | 100 | 58 | 33 | 4.2 ± 0.4 | 47.2 ± 7.5 | 16.9 ± 2.3 |
| | U73122 2.5μM | 30 | 13 | - | 1 ± 0.2 | | |
| | U73122 3.3μM | 25 | 16 | - | 1 ± 0.3 | | |
| | U73122 5μM | 0 | - | - | - | | |
| Ag | 2-APB | 95.8 | 86 | 84 | 1.6 ± 0.2 | 25.9 ± 4 | 27.5 ± 2.7 |
| | sphingosine | 26.9 | 15 | 75 | 4.4 ± 0.8 | 27.8 ± 4.7 | 49.8 ± 5.7 |
| | DM-sphingosine | 62.1 | 15 | 33 | 2.8 ± 0.5 | 41.2 ± 9 | 29.3 ± 6.3 |
| | Nifedipine | 91 | 93 | 43 | 4.6 ± 0.3 | 26.8 ± 3.8 | 12.8 ± 0.8 |
| | 1μM $Gd^{3+}$ | 80 | 87 | 69 | 3.7 ± 0.7 | 40.1 ± 6.2 | 22.7 ± 2.9 |
| | 10μM $Gd^{3+}$ | 80.8 | 89 | 50 | 1.8 ± 0.1 | 21.4 ± 3 | 20.8 ± 2.3 |

[a] Unless otherwise stated Ag was used at 1700ng/ml; number of cells in each experiment was 16-80 as specified in text or figure legends

[b] During first two minutes of response

* Data are mean ± SEM